Modulation of inwardly rectifying currents in rat sympathetic neurones by muscarinic receptors

Hong-Sheng Wang and David McKinnon

Department of Neurobiology and Behavior, State University of New York at Stony Brook, Stony Brook, NY 11794-5230, USA

1. Intracellular recordings were made from rat sympathetic neurones in isolated superior cervical ganglia (SCG), coeliac ganglia (CG), and superior mesenteric ganglia (SMG).

2. Following classification of the firing properties of these neurones as either 'phasic' or 'tonic', single-electrode voltage-clamp recordings of the inwardly rectifying current were performed. The inward rectifier conductance was 6·4 times larger in tonic neurones than in phasic neurones.

3. The basic features of the inward rectifier in sympathetic neurones were similar to those of the classic inward rectifier described in several neuronal and non-neuronal preparations. The properties of the native channel were also similar to a subset of recently cloned inwardly rectifying channels. The reversal potential and the slope conductance were both dependent on external potassium ion concentration. The conductance was blocked by low concentrations of external Ba^{2+} and Cs^{+} ions.

4. A striking feature of the inward rectifier in sympathetic neurones was its modulation by muscarine. Application of 20 μM muscarine produced a mean 78 $\pm$ 1·4% inhibition of the current. From dose–response curves for muscarine a mean dissociation constant of $K_D = 1{\cdot}95 \pm 0{\cdot}2$ μM was determined. Schild plot analysis using the competitive antagonists pirenzepine and himbacine indicated that the effect of muscarine was mediated by the M_1 class of muscarinic receptors.

5. The inward rectifier was also inhibited by repetitive nerve stimulation which produced a block of the conductance similar to that seen in response to bath-applied muscarine. The onset of inhibition was relatively slow, 20–30 s, suggesting that it is mediated by a soluble second messenger pathway.

There are distinct differences in the intrinsic electrophysiological properties of neurones found in the pre- and paravertebral sympathetic ganglia of mammals. These differences may contribute to the different functional roles of neurones in the peripheral sympathetic nervous system (Janig & McLachlan, 1992). Two basic electrophysiological types of sympathetic neurones can be identified: neurones that respond with transient bursts of action potentials (phasic neurones) or neurones that fire continuously (tonic neurones) in response to a maintained depolarizing stimulus (Weems & Szurszewski, 1978; Cassell, Clark & McLachlan, 1986; Wang & McKinnon, 1995). In the rat, neurones in the superior cervical ganglia (SCG), which is a paravertebral ganglia, have exclusively phasic firing properties (Brown & Constanti, 1980; Wang & McKinnon, 1995). The two prevertebral ganglia used in this study, the superior mesenteric ganglia (SMG) and the coeliac ganglia (CG) contain a mixture of phasic and tonic neurones. The SMG contains predominantly tonic neurones (~85%) and the CG contains approximately 60% tonic neurones (Wang & McKinnon, 1995).

We have previously shown that the presence of the M-current in phasic neurones and its relative absence in tonic neurones is a primary determinant of the switch between phasic and tonic firing properties in rat sympathetic neurones (Wang & McKinnon, 1995). In addition to the differences in M-channel expression there are co-ordinate changes in the expression of other potassium currents found in these neurones (Wang & McKinnon, 1995). In this paper we describe differences in the level of expression of the inwardly rectifying current in phasic and tonic neurones. The expression of this currrent is negatively correlated with expression of the M-channel, and this may reflect the contrasting functions of the two currents in sympathetic neurones. We also show that the inwardly rectifying channel in sympathetic neurones is dramatically inhibited by muscarinic agonists with an M_1 pharmacology.

METHODS

Electrophysiological recording

Sympathetic ganglia were obtained from young adult Sprague–Dawley rats (4–5 weeks). The superior cervical, the right coeliac and the right superior mesenteric ganglia were used in this study. These ganglia are relatively discrete in the rat and can be routinely identified for dissection (Schmidt, Modert, Yip & Johnson, 1983). Rats were anaesthetized, either with ether or urethane (1·25 g kg^{-1} I.P.), then decapitated and the ganglia quickly dissected out and placed in recording solution. The ganglia were pinned out on a strip of Sylgard in a small Lucite bath (Datyner, Gintant & Cohen, 1985). Recordings were performed at room temperature (22 °C).

The standard extracellular recording solution contained: 133 mM NaCl, 4·7 mM KCl, 1·3 mM NaH_2PO_4, 16·3 mM $NaHCO_3$, 2 mM $CaCl_2$, 1·2 mM $MgCl_2$ and 1·4 g l^{-1} glucose, bubbled with 95% O_2–5% CO_2 to give pH 7·2–7·4. Intracellular electrodes were filled with 1 M KCl and typically had resistances in the range 80–100 MΩ.

Single-electrode current and voltage-clamp recordings were performed using an Axoclamp 2A (Axon Instruments) with switching frequencies of 1·5–3 kHz. Electrode voltage during switching clamp was constantly monitored for adequate settling (Finkel & Redman, 1984). Data collection and analysis were performed using Axoclamp software (Axon Instruments). Several criteria were used for acceptance of a cell for analysis: membrane potential negative to −45 mV, input impedance greater than 80 MΩ, spike overshoot greater than 25 mV and a clear after-hyperpolarization following a single spike. Cells were held for at least 30 min. Most cells were significantly better than these minimum acceptance criteria. Mean values (± S.E.M.) for resting membrane potential and input resistance were −55 ± 1·4 mV and 173 ± 11 MΩ, respectively.

Drug concentrations, when used, were: 0·5–400 μM muscarine; 10–300 nM pirenzepine (all from Sigma) and 0·3–3 μM himbacine (gift from W. C. Taylor, University of Sydney, Australia).

Leakage subtraction and curve fitting

For all the voltage-clamp data (except the experiments shown in Fig. 4) leakage subtraction was performed by first fitting the following equation:

$$I = G_{IR}(V_m - E_K)/\{1 + \exp((V_m - V_{½})/k)\} + G_L(V_m - E_L), \quad (1)$$

where G_{IR} is the maximum inward rectifier conductance; V_m is the membrane potential; E_K is the Nernst potential for K^+; $V_{½}$ is the voltage at which the inward rectifier conductance is half-maximal; k is a measure of the rate at which the conductance changes with voltage; G_L is the linear leakage conductance; and E_L is the reversal potential for the leak conductance. Equation (1) was fitted by least-squares minimization using the Solve function in Excel (Microsoft). For fitting, E_K was set to −90 mV and all the other parameters were left free. The fitting procedure converged consistently on the same result independent of starting parameters and none of the free parameters showed unusual variability (see Table 1). The linear leakage current was subtracted from the records.

This procedure was not used for the Ba^{2+} and Cs^+ block experiments (Fig. 4) because the voltage dependence of the cation block required a more complex equation to fit the data. For these data, rather than introduce futher variables into the fitted equation, we subtracted the leakage current produced by a step from −60 to −70 mV after appropriate scaling. This procedure introduces a small systematic error into the data by subtracting a small fraction of the inwardly rectifying current. It has the advantage of adjusting for any block of the leak conductance by the cations. The systematic error becomes smaller at higher cation concentrations as the inward rectifier is blocked and should not, therefore, greatly influence the interpretation of the data.

Nerve stimulation experiments

The greater splanchnic nerve trunk was dissected out together with the coeliac ganglia. Nerve stimulation was performed using close-fitting suction electrodes (A-M Systems, Inc., Everett, WA, USA), with 0·5 ms square pulses and suprathreshold stimulus intensities of 20–100 V. In some experiments synaptic stimulation produced a shift in the potassium reversal potential, presumably due to simultaneous activation of large numbers of neurones and consequent potassium accumulation in the extracellular space. Blockade of nicotinic inputs with 0·4 mM curare eliminated this shift. Significant shifts in the reversal potential were not seen in all cells and appeared to be related to the cells position in the ganglia. No difference in the effect of synaptic stimulation on the inward rectifier was found when curare was used.

Schild plot analysis

The method of Arunlakshana & Schild (1959) was used to determine the affinities of muscarinic receptor antagonists. Dose–response relationships for the inhibition of the inward rectifier by muscarine were obtained in the absence and then in the presence of various concentrations of antagonist. Drugs were perfused for 5–10 min and two or three voltage step protocols were performed at each concentration of agonist and antagonist to ensure that the drug effect had reached steady state. The control data points were fitted with the Hill equation. After each dose–response curve was measured, cells were washed for 1 h to allow full recovery of the inward rectifier before a second dose–response curve was obtained. There was no reduction of the inward rectifier conductance in control solutions between trials. A percentage of inhibition within the steep region of the dose–response curve was chosen (normally half of the maximum suppression), and the ratio of muscarine concentration required to produce the chosen percentage of inhibition in the presence and absence of antagonist was calculated as the dose ratio. Dose ratios were plotted on a Schild plot and were fitted with lines constrained to a slope of unity. Intercepts of the lines yield estimated pK_B values (−log of dissociation constant) (Jenkinson, 1991), and the results were compared with the published data for antagonist affinities for different muscarinic receptor subtypes (Table 2).

RESULTS

Differential expression of the inwardly rectifying current in phasic and tonic neurones

Phasic and tonic neurones were distinguished by their response to depolarizing current steps. As described previously (Wang & McKinnon, 1995), phasic neurones respond to a current step with one, or a few, action potentials at the start of a current step and do not fire subsequent action potentials. In contrast, tonic neurones fire continuous action potentials in response to a suprathreshold stimulus.

There are marked differences in the steady-state I–V relationship of the two cell types (Fig. 1*A*). The difference

Table 1. Comparison of inward rectifier and leakage current properties in phasic and tonic neurones

	G_{IR} (pS pF^{-1})	$V_{½}$ (mV)	k (mV)	G_L (nS)	E_L (mV)
Tonic nuerones	345 ± 20	−103 ± 1·4	11·2 ± 0·4	8·2 ± 0·4	−39 ± 1·7
Phasic neurones	54 ± 12	−103 ± 4·5	10·0 ± 0·07	8·4 ± 0·9	−37 ± 4·0
Tonic/phasic	6·4	1·01	1·12	0·99	1·06

Data are expressed as means ± S.E.M. with $n = 25$ for tonic neurones and $n = 11$ for phasic neurones. G_{IR} in tonic cells was significantly larger than in phasic neurones ($P < 0·0001$). There was no statistically significant difference for any other parameters ($P > 0·3$). The value for G_{IR} is the specific conductance, which corrects for the small difference in the mean cell membrane capacitance between tonic (124 ± 6 pF) and phasic (147 ± 17 pF) neurones. Tonic neurones were recorded in the SMG and CG and phasic cells were recorded in all three ganglia.

in the response to depolarizing current steps is largely due to the M-current, which is only found in phasic neurones (Wang & McKinnon, 1995). The difference in the response to hyperpolarizing current steps is due to the presence of a larger inwardly rectifying current in tonic neurones than in phasic neurones. In tonic neurones, hyperpolarizing voltage steps negative to −90 mV evoked large inward currents (Fig. 1*B*). This inwardly rectifying current reached a peak within 10–20 ms and then declined slightly to a maintained steady-state level. Phasic neurones also showed inward rectification but the average size of the currents was much smaller (Fig. 1*B*).

The current–voltage curve of the inward rectifier could be fitted using eqn (1) (Fig. 2*A*; Hagiwara & Takahashi, 1974). The maximum conductance of the inwardly rectifying current was determined using eqn (1). For tonic cells in the SMG and CG, the maximum conductance was relatively large, with a mean value of 41·9 ± 2·6 nS, and the conductance density was 345 ± 20 pS pF^{-1} ($n = 25$). In marked contrast, the inwardly rectifying current was significantly smaller in phasic neurones found in the SCG, CG and SMG, with a mean maximum conductance of 7·9 ± 1·7 nS and a conductance density of 54 ± 12 pS pF^{-1} ($n = 11$). The average inward rectifier conductance density was 6·4 times larger in tonic neurones than in phasic neurones (Table 1). There was no overlap in the distributions of the specific conductance between phasic and tonic neurones (Fig. 2*B*). There was no significant difference in the values for $V_{½}$ or k between phasic and tonic neurones and the properties of the linear leakage conductance was the same in both sets of neurones (Table 1). The values for $V_{½}$ and k were similar to those described in other mammalian neurones (Stanfield, Nakajima & Yamaguchi, 1985; Uchimura & North, 1990).

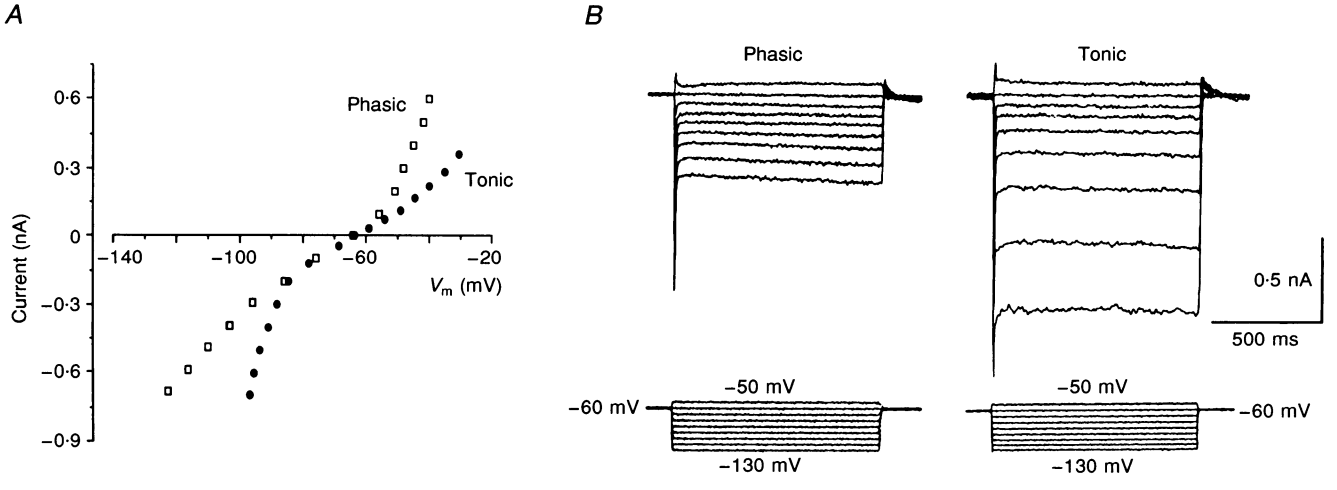

Figure 1. Inward rectification in phasic and tonic sympathetic neurones

A, steady-state current–voltage relationship of a phasic and a tonic neurone with similar input resistances. Data points are from recordings made in current-clamp mode in which the steady-state voltage was measured 500 ms after the onset of a current step. *B*, voltage-clamp analysis of inwardly rectifying currents in a phasic neurone (left) and a tonic neurone (right), both from the SMG. Upper traces, current; lower traces, voltage. Recordings show current responses to voltage steps over the range −130 to −50 mV, in 10 mV increments, from a holding potential of −60 mV. Currents are shown without subtraction of linear leakage currents.

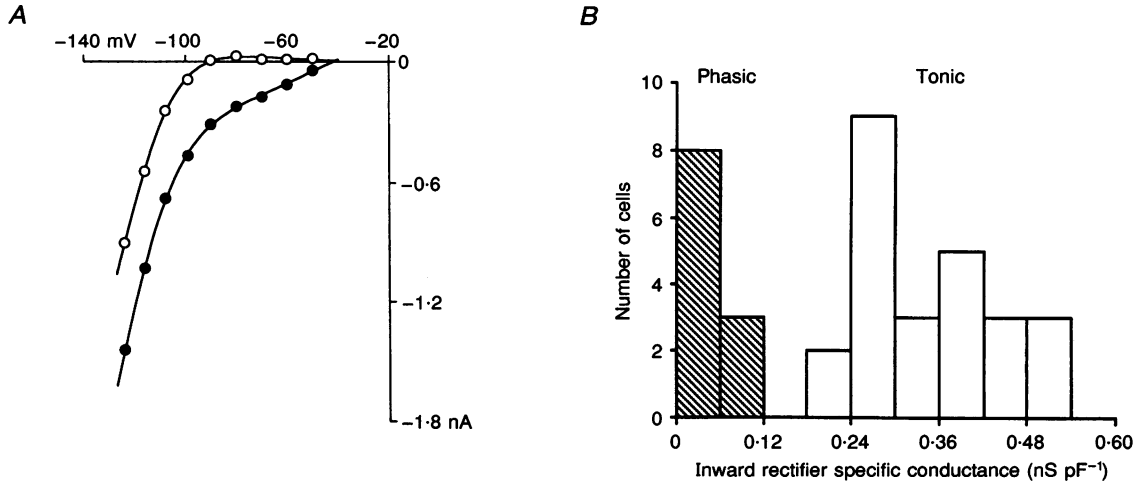

Figure 2. Comparison of inwardly rectifying current densities in tonic and phasic neurones

A, *I–V* curves for the tonic cell shown in Fig. 1*B* before (●) and after (○) subtraction of the linear leak current (see Methods for details). Currents were measured 10 ms after the capacitance artifact and were fitted using eqn (1), where $G_{IR} = 36{\cdot}8$ nS, $V_{½} = -113{\cdot}4$ mV, $k = 11{\cdot}4$ mV, $G_L = 6{\cdot}6$ nS, and $E_L = -42{\cdot}1$ mV. E_K was set to −90 mV. The curve through the subtracted data points (○) is described by the equation: $I_{IR} = G_{IR}(V_m - E_K)/\{1 + \exp((V_m - V_{½})/k)\}$, with the same parameter values as for the unsubtracted data points. *B*, histogram of the distribution of values for the inward rectifier specific conductance in phasic and tonic neurones.

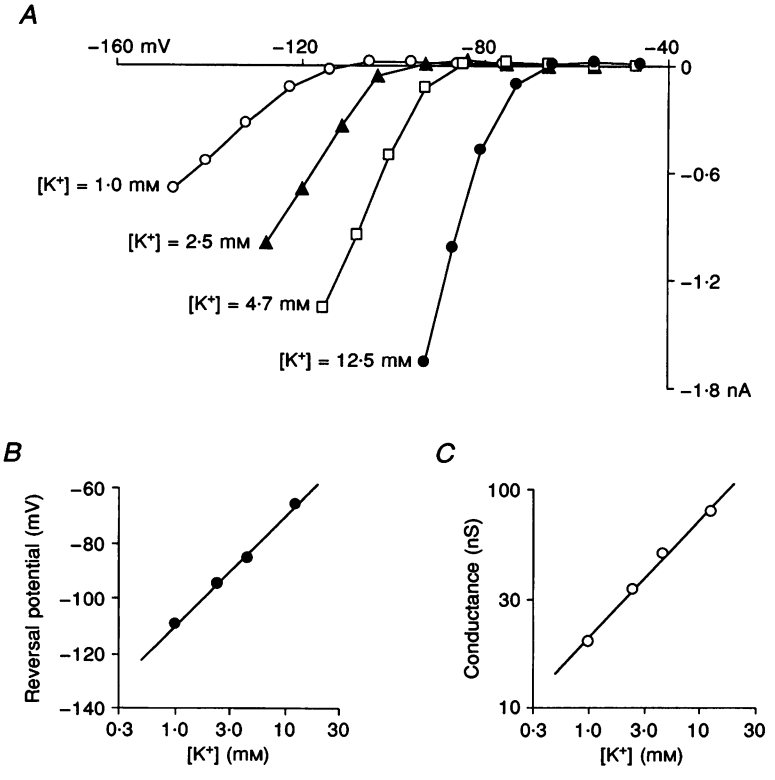

Figure 3. Effect of external potassium ion concentration on reversal potential and conductance

A, *I–V* relationship of the inward rectifier in different external potassium ion concentrations. Data points are shown following subtraction of linear leak currents and were fitted with eqn (1) allowing E_K to vary (see Methods for details). *B*, dependence of reversal potential on external potassium ion concentration. *C*, dependence of slope conductance on external potassium ion concentration. All the data shown in this figure were obtained from a tonic neurone in the SMG.

Characteristics of the inwardly rectifying current in tonic neurones

Tonic neurones proved to be a favourable neuronal preparation for the study of the inward rectifier and we were able to obtain a relatively detailed description of the properties of this current to compare with the properties of cloned inwardly rectifying channels (Kubo, Baldwin, Jan & Jan, 1993; Perier, Radeke & Vandenberg, 1994; Makhina, Kelly, Lopatin, Mercer & Nichols, 1994). One characteristic property of inwardly rectifying potassium currents is the dependence of the reversal potential on E_K (Hagiwara, Miyazaki & Rosenthal, 1976). Raising the external $[K^+]$ from 1·0 mM to 2·5, 4·7, and 12·5 mM, shifted the reversal potential to progressively more positive potentials (Fig. 3*A*),

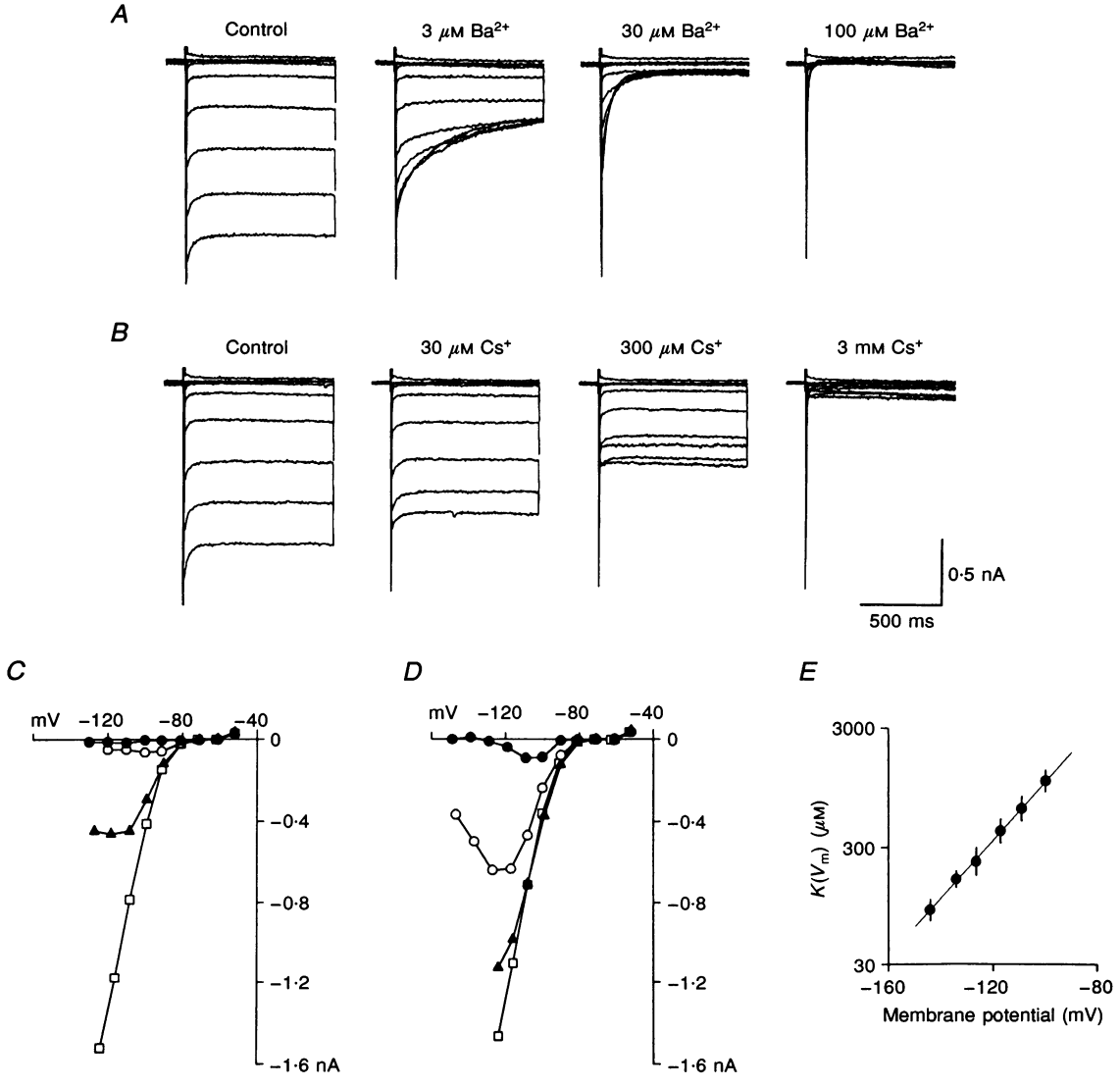

Figure 4. Block of inwardly rectifying currents by external cations

A, block of inwardly rectifying currents by external barium ions. *B*, block of inwardly rectifying currents by external Cs^+. In both *A* and *B* the records show current responses to voltage steps in 10 mV increments from a holding potential of −60 mV. *C*, steady-state *I–V* relationships of inward rectifier in 0 μM (□), 3 μM (▲), 30 μM (○), and 100 μM external Ba^{2+} (●). *D*, *I–V* relationships of inward rectifier in 0 μM (□), 30 μM (▲), 300 μM (○), and 3 mM external Cs^+ (●). Current amplitudes at the end of the 1000 ms voltage steps or at the start of the voltage steps (10 ms after the capacitance artifact) were plotted in *C* or *D*, respectively. *E*, voltage dependence of Cs^+ block. Plot of the mid-point for Cs^+ block, $K(V_m)$, as a function of membrane potential, V_m. The data points are means from three cells and were fitted with the equation $K(V_m) = K(0)\exp(\delta FV_m/RT)$, where δ is the apparent fraction of the membrane field sensed by the blocking ion, $K(0)$ is the Cs^+ concentration causing half-maximal block at 0 mV, and *F*, *R* and *T* have their usual meaning. The fitted parameters were $\delta = 1{\cdot}5$ and $K(0) = 353$ mM. Vertical bars are S.E.M. Both the current records and the data points are shown following subtraction of linear leak currents using the procedure described in the Methods section. These data were obtained from tonic neurones in the SMG.

as expected for a typical inward rectifier. The mean value for the shift in the reversal potential per 10-fold change in external $[K^+]$ was 53 ± 5 mV (Fig. 3*B*), which is in reasonable agreement with the prediction from the Nernst equation. The slope conductance of the inward rectifier also depended on external K^+ concentration. A double-logarithmic plot of slope conductance against external $[K^+]$ showed a linear relationship (Fig. 3*C*) with a mean slope of $0{\cdot}5 \pm 0{\cdot}01$, consistent with a multi-ion pore (Hille & Schwarz, 1978). It is a feature of many inward rectifiers that the conductance is approximately proportional to the square root of external $[K^+]$ (Hagiwara & Takahashi, 1974) and the cloned IRK1 channel has a similar dependency (Kubo *et al.* 1993).

Blockade by external cations

The sensitivity of the inwardly rectifying current to block by external cations was also examined. The inwardly rectifying current in tonic neurones was very sensitive to external Ba^{2+} and the blockage was time and voltage dependent (Fig. 4*A* and *C*). In the presence of low concentrations of Ba^{2+} (1–3 μM), the inward current was affected only at very hyperpolarized potentials. Upon activation, the inward current reached peak amplitude instantaneously and declined slowly to a markedly reduced steady-state level. When the concentration of Ba^{2+} was raised to 100–300 μM, both the instantaneous and the steady-state component of the inward current were totally abolished (Fig. 4*A* and *C*).

The inward current was also sensitive to external Cs^+ (Fig. 4*B* and *D*). The block of the inward current by Cs^+ was voltage and concentration dependent, but had little time dependence. The dissociation constant for Cs^+ block, $K(V_m)$, was determined at each membrane potential and a plot of the logarithm of $K(V_m)$ as a function of membrane potential was linear (Fig. 4*E*). The voltage dependence of the $K(V_m)$ can be described by the following equation,

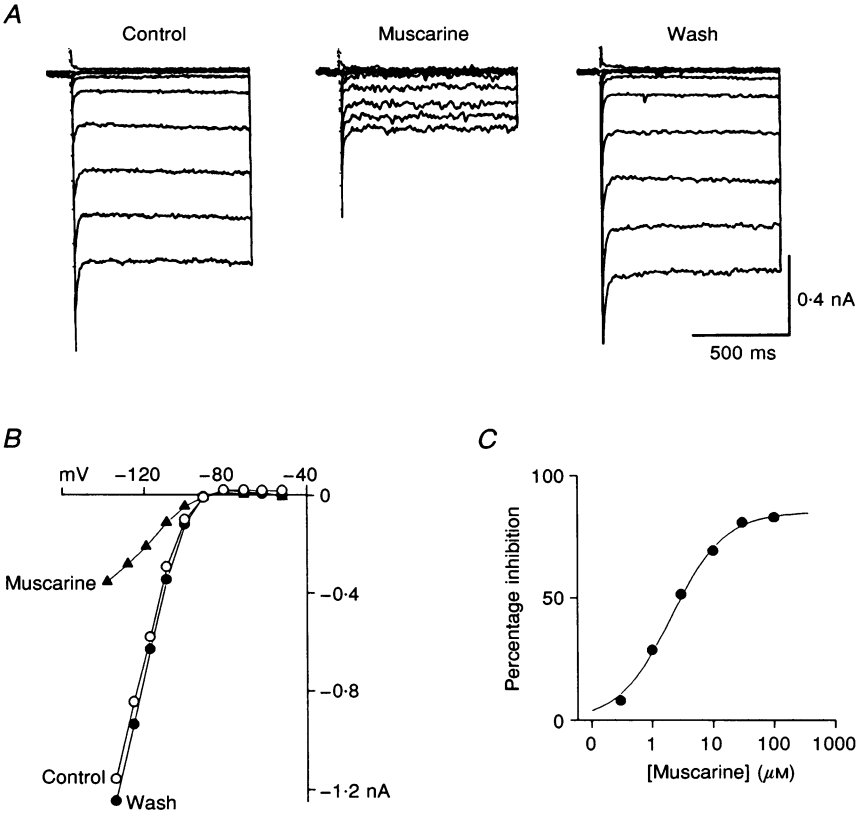

Figure 5. Suppression of the inwardly rectifying current by muscarine

A, block of inwardly rectifying currents by 20 μM muscarine and subsequent washout. The records show current responses to voltage steps over the range −140 to −50 mV, in 10 mV increments, from a holding potential of −60 mV. *B*, *I–V* curve before, during and after washout of 20 μM muscarine. Current records and data points are shown following subtraction of linear leak currents using the procedure described in the Methods section. *C*, dose–response curve for muscarine inhibition of the inward rectifier in a tonic neurone. Data points were fitted using the Hill equation:

$$\text{Percentage inhibition} = \text{maximum inhibition}(1/(1 + (K_D/[\text{muscarine}]))),$$

with $K_D = 2{\cdot}1$ μM and a maximum inhibition = 85%. Recordings were obtained from tonic neurones in the SMG.

which assumes a single binding site in the pore of the channel (Woodhull, 1973):

$$K(V_m) = K(0)\exp(\delta F V_m/RT), \quad (2)$$

where δ is the apparent fraction of the membrane field sensed by the blocking ion; $K(V_m)$ and $K(0)$ are the Cs^+ concentrations causing half-maximal block at V_m and 0 mV, respectively; V_m is the membrane potential; and F, R and T are the usual thermodynamic quantities. The value for the apparent fraction of the membrane field sensed by Cs^+ was greater than one ($\delta = 1{\cdot}46 \pm 0{\cdot}02$, $n = 3$), suggesting that there are multiple binding sites for Cs^+ within the membrane electric field (Hagiwara *et al.* 1976). The value for δ is very similar to the values found for Cs^+ blockade of the cloned IRK family of inwardly rectifying channels (1·53: Kubo *et al.* 1993; 1·4: Perier *et al.* 1994; 1·46: Makhina *et al.* 1994).

Inhibition of the inward rectifier by muscarine

One unusual property of the inwardly rectifying current in both phasic and tonic neurones was its inhibition by low concentrations of muscarine (Fig. 5). The pharmacology of this inhibition was studied in detail in tonic neurones, where the currents were larger and easier to study in isolation. Application of 20 μM muscarine by bath perfusion for 5–10 min inhibited the inwardly rectifying current by 78 ± 1·4% ($n = 10$). The remaining current was blocked by 100 μM Ba^{2+} (data not shown). From dose–response curves for muscarine inhibition (Fig. 5*C*) an average dissociation constant, $K_D = 1{\cdot}95 \pm 0{\cdot}2$ μM ($n = 5$), and a maximum inhibition of 84 ± 1·2% were determined. The current always recovered fully following washout of muscarine (Fig. 5*A*). In a few cells (2 out of 15) there was no effect of muscarine on the current. Whether this was due to an absence of the appropriate subclass of muscarinic receptor on these cells or was due to cell damage following the electrode impalement was not determined.

The muscarinic receptor subtype responsible for the suppression of this current was determined by Schild plot analysis of the actions of two partially selective antagonists, pirenzepine and himbacine. A dose–response curve for muscarine was obtained in the absence and then the presence of different concentrations of pirenzepine

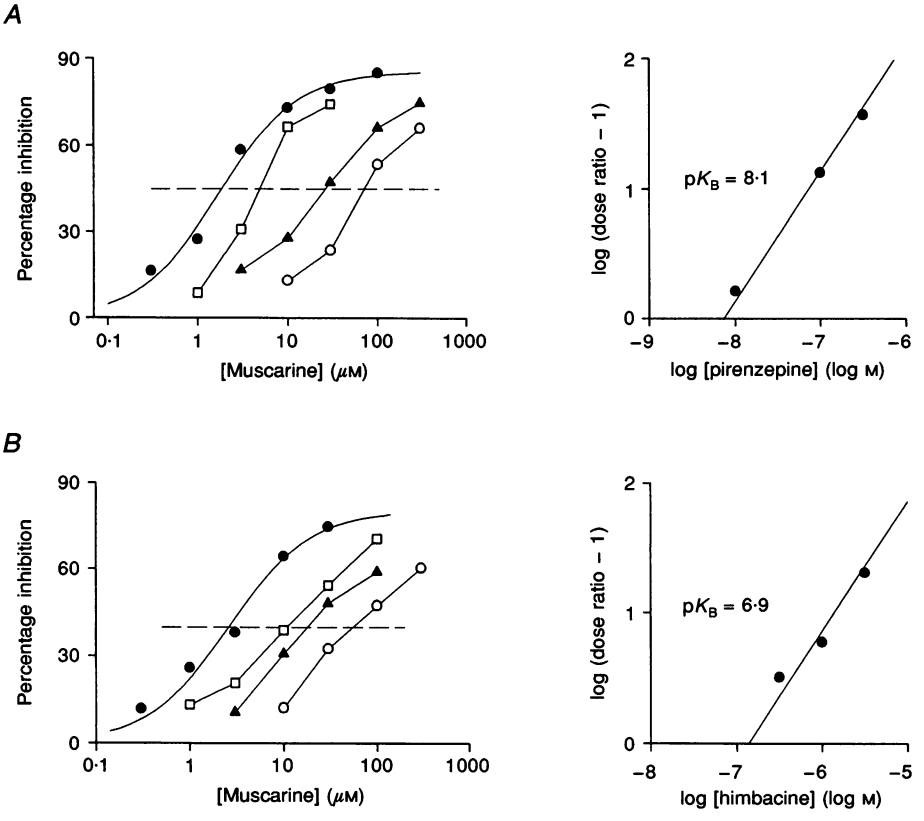

Figure 6. Pharmacological profile of muscarinic suppression of the inward rectifier

A, left: competitive shift of muscarine dose–response curve by 0 nM (●), 10 nM (□), 100 nM (▲) and 300 nM pirenzepine (○). *A*, right: Schild plot of pirenzepine antagonism of the muscarinic effect in the same cell. The dose ratios for muscarine suppression of the inwardly rectifying current were fitted with a line constrained to a slope of unity to give an estimated pK_B value (see Methods). *B*, left: competitive shift of muscarine dose–response curve by 0 nM (●), 300 nM (□), 1 μM (▲) and 3 μM himbacine (○). *B*, right: Schild plot analysis of himbacine antagonism of the muscarinic effect on the inward rectifier.

Table 2. Comparison of antagonist potencies for muscarinic inhibition of inward rectifier with muscarinic receptor subtype pK_B values

		pK_B values for muscarinic receptor subtypes*				
	pK_B	m1	m2	m3	m4	m5
Pirenzepine	8·1 ± 0·1	8·0 ± 0·1	6·3 ± 0·1	6·9 ± 0·1	7·4 ± 0·2	7·1
Himbacine	6·9	7·1 ± 0·1	8·2 ± 0·2	7·1 ± 0·1	8·3 ± 0·2	6·4 ± 0·2

* Data are means ± S.E.M. from previously published binding and functional studies: Fukuda, Kubo, Akiba, Maeda, Mishina & Numa (1987); Akiba *et al.* (1988); Buckley, Bonner, Buckley & Brann (1989); Lazareno, Buckley & Roberts (1990); Dorje, Wess, Lambrecht, Tacke, Mutschler & Brann (1991); Caulfield & Brown (1991); Miller, Aagaard, Gibson & McKinney (1992).

(Fig. 6*A*). Schild plots (Fig. 6*A*) of the mid-point for muscarinic suppression at different pirenzepine concentrations produced a mean pK_B for pirenzepine of 8·1 ± 0·1 ($n = 3$). This value is most consistent with the muscarine response being mediated by the M_1 subtype of muscarinic receptors (Table 2). A contribution by M_4 receptors cannot be completely excluded by the use of pirenzepine by itself (Bernheim, Mathie & Hille, 1992; Caulfield, Robbins, Higashida & Brown, 1993). To distinguish between M_1 and M_4 receptors the antagonist himbacine was used (Fig. 6*B*). The pK_B for himbacine was 6·9 ($n = 2$) which is also consistent with M_1 pharmacology and is inconsistent with M_4 pharmacology (Table 2). It is most likely, therefore, that the majority of the effect of muscarine on the inward rectifier in these neurones is mediated by the M_1 subtype of muscarinic receptors.

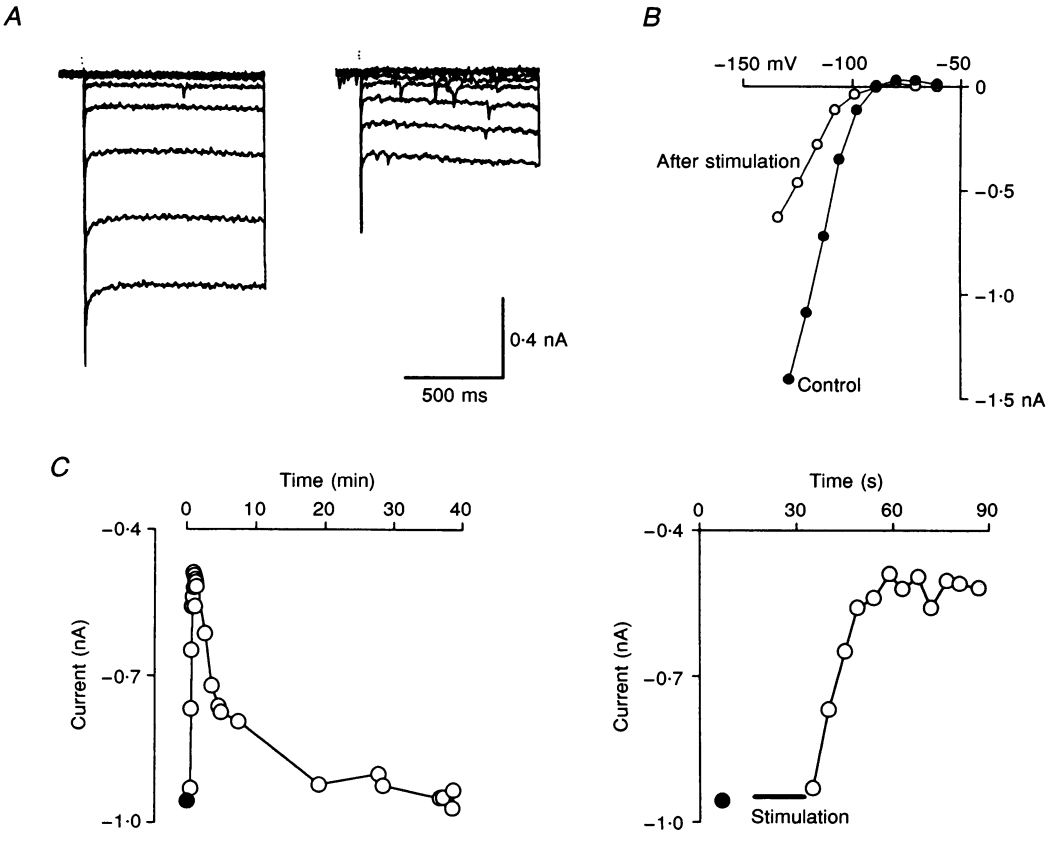

Figure 7. Effect of repetitive nerve stimulation on the inward rectifier

A, inwardly rectifying currents before and after repetitive stimulation of the greater splanchnic nerve (10 s at 30 Hz) showing significant suppression of the inward rectifier following nerve stimulation. The records show current responses to voltage steps over the range −130 to −50 mV, in 10 mV increments, from a holding potential of −60 mV. *B*, *I–V* curve before and after nerve stimulation. Current records and data points are shown following subtraction of linear leak currents using the procedure described in the Methods section. *C*, time course of inward rectifier suppression following repetitive nerve stimulation. Note the different time scales. This data was obtained from tonic neurones in the CG.

Inhibition of inward rectifier by synaptic stimulation

Inhibition of the inward rectifier could also be mediated by synaptic stimulation. Recordings of the inwardly rectifying current were made from tonic neurones in the coeliac ganglia before and after stimulation of the splanchnic nerve. Repetitive stimulation of the greater splanchnic nerve produced significant suppression of the inward rectifier (Fig. 7). This synaptically mediated suppression was blocked by 1 μM atropine (data not shown).

The time course of suppression of the inwardly rectifying current was examined using nerve stimulation. Relatively brief stimulations (10–15 s) produced a significant depression of the inwardly rectifying current (Fig. 7*C*). The onset of the suppression of the inward rectifier appeared to involve a significant delay and typically took 20–30 s to reach a peak following the cessation of nerve stimulation. The relatively slow effect of synaptically released acetylcholine suggests that it is mediated by a soluble second messenger pathway. Recovery began ~1·5 min after cessation of the stimulus and full recovery took 10–20 min.

Physiological function of the inward rectifier in tonic neurones

One function of the large inwardly rectifying current in tonic neurones may be to provide a steady potassium conductance that helps maintain the resting membrane potential. In our previous computer modelling studies of sympathetic neurones (Wang & McKinnon, 1995), we found that the model tonic neurone tended to be unstable in the voltage range between the resting membrane potential and threshold. The model tonic neurone lacked significant non-inactivating outward currents between −65 and −45 mV and was easily depolarized by small prolonged currents. Phasic neurones, in contrast, were stabilized in this region by the M-current. The activation curve of the M-current starts around the resting membrane potential and depolarizing currents tend to activate this conductance, which makes these cells relatively stable in response to small depolarizing stimuli. In the model tonic neurone a significant steady-state linear leak conductance was necessary to stabilize the membrane potential to small current perturbations. Although this was not unrealistic in terms of our experimental data, it is possible that at least part of the experimentally observed leak conductance is artifactual, due to microelectrode impalement. In intact tonic neurones, the inward rectifier probably makes a contribution to the resting potassium conductance responsible for maintenance of the resting membrane potential.

It was possible to demonstrate experimentally the contribution of the inward rectifier to the resting membrane potential of tonic neurones by examining the effect of a low concentration of Ba^{2+} ions on the membrane potential at different holding potentials (Fig. 8). Application of 300 μM Ba^{2+} produced a significant depolarization of tonic neurones over the normal range of resting membrane potentials (Fig. 8*A*). The reversal potential for this effect was close to E_K (~−92 mV) and the voltage change produced by Ba^{2+} application became much larger at hyperpolarized potentials, as expected for a specific blockade of the inward rectifier (Fig. 8*B*).

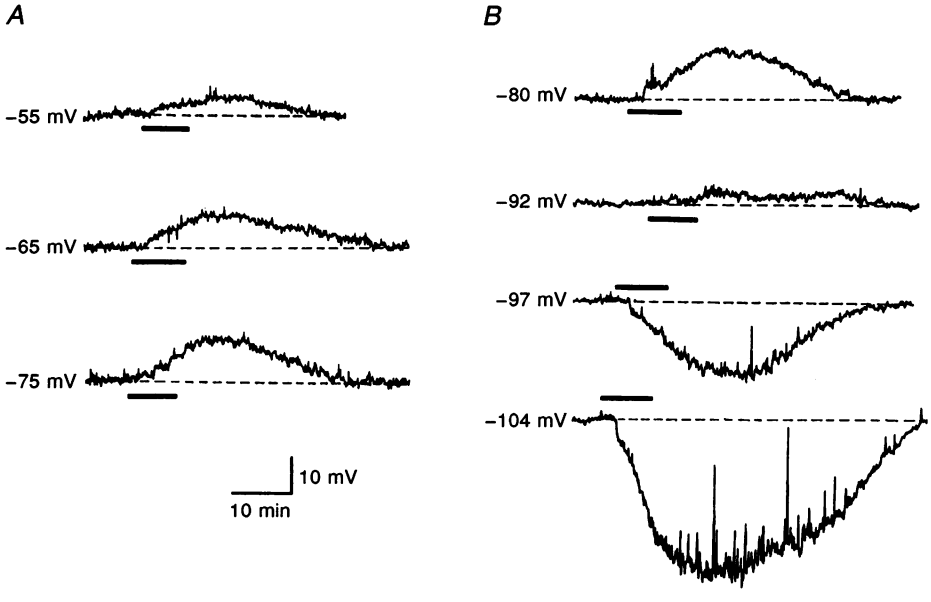

Figure 8. Effect of external barium ions on the membrane potential of a tonic neurone

A, the effect of 300 μM Ba^{2+} on the membrane potential at different holding potentials. The initial resting potential in this neuron was −60 mV. *B*, the reversal potential for the effect of 300 μM Ba^{2+} on membrane potential is close to −90 mV. Recordings were obtained from a tonic neurone in the SMG. The bar indicates the duration of Ba^{2+} application.

Another function of the M-current in phasic cells is the generation of the slow EPSP, which is produced, in part, by muscarinic receptor mediated inhibition of the M-current (Brown, 1988). Inhibition of the inward rectifier may also contribute to the slow muscarinic EPSP seen in tonic neurones, but there are clearly other currents that are also important (H.-S. Wang & D. McKinnon, unpublished data; cf. Brown & Selyanko, 1985).

DISCUSSION

In this paper we show that the expression of the inwardly rectifying current in rat peripheral sympathetic neurones is strongly correlated with intrinsic firing properties. Tonic sympathetic neurones express a significantly larger inward rectifier conductance than do phasic neurones and there is no overlap of the distribution of this conductance between the two cell types. The difference in the size of this conductance can account for the different I–V curves that these cells display at hyperpolarized membrane potentials. In guinea-pigs, inward rectification is also generally larger in tonic than phasic sympathetic neurones (Cassell *et al.* 1986), suggesting that this is a general feature of the peripheral sympathetic nervous system.

The inwardly rectifying current found in rat sympathetic neurones has very similar properties to the IRK family of inward rectifiers, including the dependence of the conductance on external K^+ concentration, blockade by Cs^+ and Ba^{2+} ions and its kinetic properties (Kubo *et al.* 1993; Perier *et al.* 1994; Makhina *et al.* 1994). The native channel appears to belong to the 'strongly' rectifying class of inward rectifiers rather than the 'mildly' rectifying channels typified by the ROMK1 class of inward rectifiers (Hille, 1992; Makhina *et al.* 1994). In a parallel study we have shown that mRNA encoding some members of the IRK gene family is expressed in the sympathetic ganglia (J. E. Dixon & D. McKinnon, unpublished observations), which is consistent with the idea that the native channel is encoded by the IRK genes, but further work is required to establish this relationship.

The inwardly rectifying current in sympathetic neurones is dramatically inhibited by activation of the M_1 muscarinic receptors and this modulation can also be produced by repetitive nerve stimulation. A reduction of the inwardly rectifying current by muscarine has been reported previously in rat nucleus accumbens neurones (Uchimura & North, 1990), although the maximal reduction by muscarine in these cells was relatively small (~22% reduction). Substance P (Stanfield *et al.* 1985) and 5-hydroxytryptamine (North & Uchimura, 1989) have been reported to reduce the inward rectifier in other mammalian neurones. Activation of M_1 receptors has previously been shown to modulate both the M-current and the L-type calcium current in sympathetic neurones (Bernheim *et al.* 1992; Caulfield *et al.* 1993). This signalling pathway is thought to require a soluble second messenger and has a relatively long latency (10–60 s: Hille, 1994). Modulation of the inward rectifier in sympathetic neurones is also relatively slow (20–30 s), suggesting that the same second messenger pathway is also responsible for suppression of the inward rectifier in sympathetic neurones.

It is notable that the inward rectifier and the M-current have opposite distributions in tonic and phasic neurones, suggesting that they may have distinct, but related, functions in the two cell types. The inward rectifier contributes to the maintenance of the resting membrane potential in the region between resting potential and threshold. This is similar to the function of the M-current, which also acts to stabilize the resting membrane potential (Brown, 1988). However, the activation properties of the M-current make it considerably more effective in clamping the membrane potential below threshold during maintained depolarizing currents. Inhibition of the inward rectifier by muscarinic receptor activation increases electrical excitability in tonic neurones by reducing the resting potassium conductance, in much the same way that inhibition of the M-current does in phasic neurones (Brown & Selyanko, 1985). In addition, inhibition of both channels is mediated by M_1 muscarinic receptors and may contribute to the slow EPSP (Marrion, Smart, Marsh & Brown, 1989; Bernheim *et al.* 1992).

It is interesting to ask why phasic and tonic sympathetic neurones switch between high levels of expression of the M-current or the inward rectifier if these two conductances can perform overlapping functions. The answer to this question possibly relates to the nature of the synaptic input that the two cell types receive. Phasic neurones receive one or a few very large suprathreshold EPSPs that dominate the synaptic input to these neurones (Skok & Ivanov, 1983; Hirst & McLachlan, 1986). In addition, they receive a number of small, subthreshold EPSPs that cannot normally drive the cell (Skok & Ivanov, 1983). In contrast, fast synaptic input to tonic neurones is exclusively provided by small, subthreshold EPSPs that have to summate in order to fire the cell (Crowcroft, Holman & Szurszewski, 1971; McLachlan & Meckler, 1989). In rat sympathetic ganglia there is a similar correlation between the type of synaptic input that a neurone receives and the nature of its firing properties (H.-S. Wang & D. McKinnon, unpublished observations).

The different I–V relationships of the inward rectifier and M-current may affect synaptic integration in these cells. The inwardly rectifying current becomes smaller as the membrane potential approaches threshold, in marked contrast to the M-current, which is activated by depolarizing stimuli. The I–V properties of the inward rectifier probably facilitate summation of the small synaptic inputs to tonic neurones. In contrast, the properties of the M-current reduce the possibility that small EPSPs can summate and drive the phasic neurones, so that the synaptic pathway through these cells is

dominated by the suprathreshold EPSPs, which are sufficiently large and fast that they are unaffected by the presence of the M-current. What physiological function requires that sympathetic neurones have these different characterisics is not known. Potentially, the M-current participates in a gating mechanism, allowing phasic neurones to perform two types of integration on the synaptic inputs that they receive. At low stimulation frequencies the pathway through the phasic neurones is dominated by the large inputs. Following repetitive stimulation of the presynaptic nerve, and muscarinic suppression of the M-current, the small inputs may also provide significant synaptic drive to these cells. In tonic neurones, small EPSPs can summate even at low stimulation rates. Higher stimulation frequencies will probably increase the excitability of the cell by decreasing the resting potassium conductance provided by the inward rectifier.

AKIBA, I., KUBO, T., MAEDA, A., BUJO, H., NAKAI, J., MISHINA, M. & NUMA, S. (1988). Primary structure of porcine muscarinic actylcholine receptor III and antagonist binding studies. *FEBS Letters* **235**, 257–261.

ARUNLAKSHANA, O. & SCHILD, H. O. (1959). Some quantitative uses of drug antagonists. *British Journal of Pharmacology* **14**, 48–58.

BERNHEIM, L., MATHIE, A. & HILLE, B. (1992). Characterization of muscarinic receptor subtypes inhibiting Ca^{2+} and M current in rat sympathetic neurons. *Proceedings of the National Academy of Sciences of the USA* **89**, 9544–9548.

BROWN, D. A. (1988). M Currents. In *Ion Channels*, vol. 1, ed. NARAHASHI., T., pp. 55–94. Plenum, New York.

BROWN, D. A. & CONSTANTI, A. (1980). Intracellular observations on the effects of muscarinic agonists on rat sympathetic neurones. *British Journal of Pharmacology* **70**, 593–608.

BROWN, D. A. & SELYANKO, A. A. (1985). Membrane currents underlying the cholinergic slow excitatory postsynaptic potential in the rat sympathetic ganglion. *Journal of Physiology* **365**, 365–387.

BUCKLEY, N. J., BONNER, T. I., BUCKLEY, C. M. & BRANN, M. R. (1989). Antagonist binding properties of five cloned muscarinic receptors expressed in CHO-K1 cells. *Molecular Pharmacology* **35**, 469–476.

CASSELL, J. F., CLARK, A. L. & MCLACHLAN, E. M. (1986). Characteristics of phasic and tonic sympathetic ganglion cells of the guinea-pig. *Journal of Physiology* **372**, 457–483.

CAULFIELD, M. P. & BROWN, D. A. (1991). Pharmacology of the putative M_4 muscarinic receptor mediating Ca-current inhibition in neuroblastoma x glioma hybrid (NG 108-15) cells. *British Journal of Pharmacology* **104**, 39–44.

CAULFIELD, M. P., ROBBINS, J., HIGASHIDA, H. & BROWN, D. A. (1993). Postsynaptic actions of acetylcholine: the coupling of muscarinic receptor subtypes to neuronal ion channels. *Progress in Brain Research* **98**, 293–301.

CROWCROFT, P. J., HOLMAN, M. E. & SZURSZEWSKI, J. H. (1971). Excitatory input from the distal colon to the inferior mesenteric ganglion in the guinea-pig. *Journal of Physiology* **219**, 443–461.

DATYNER, N. B., GINTANT, G. A. & COHEN, I. S. (1985). Versatile temperature controlled tissue bath for studies of isolated cells using an inverted microscope. *Pflügers Archiv* **403**, 318–323.

DORJE, F., WESS, J., LAMBRECHT, G., TACKE, R., MUTSCHLER, E. & BRANN, M. R. (1991). Antagonist binding profiles of five cloned human muscarinic receptor subtypes. *Journal of Pharmacology and Experimetnal Therapeutics* **256**, 727–733.

FINKEL, A. S. & REDMAN, S. (1984). Theory and operation of a single microelectrode voltage clamp. *Journal of Neuroscience Methods* **11**, 101–127.

FUKUDA, K., KUBO, T., AKIBA, I., MAEDA, A., MISHINA, M. & NUMA, S. (1987). Molecular distinction between muscarinic acetylcholine receptor subtypes. *Nature* **327**, 623–625.

HAGIWARA, S., MIYAZAKI, S. & ROSENTHAL, N. P. (1976). Potassium current and the effect of cesium on this current during anomalous rectification of the egg cell membrane of a starfish. *Journal of General Physiology* **67**, 621–638.

HAGIWARA, S. & TAKAHASHI, K. (1974). The anomalous rectification and cation selectivity of the membrane of a starfish egg cell. *Journal of Membrane Biology* **18**, 61–80.

HILLE, B. (1992). *Ionic Channels of Excitable Membranes*, 2nd edn. Sinauer, Sunderland, MA, USA.

HILLE, B. (1994). Modulation of ion-channel function by G-protein-coupled receptors. *Trends in Neurosciences* **17**, 531–536.

HILLE, B. & SCHWARZ, W. (1978). Potassium channels as multi-ion single-file pores. *Journal of General Physiology* **72**, 409–442.

HIRST, G. D. S. & MCLACHLAN, E. M. (1986). Development of dendritic calcium currents in ganglion cells of the rat lower lumbar sympathetic chain. *Journal of Physiology* **377**, 349–368.

JANIG, W. & MCLACHLAN, E. M. (1992). Characteristics of function-specific pathways in the sympathetic nervous system. *Trends in Neurosciences* **15**, 475–481.

JENKINSON, D. H. (1991). How we describe competitive antagonists: three questions of usage. *Trends in Pharmacological Sciences* **12**, 53–54.

KUBO, Y., BALDWIN, T. J., JAN, Y. N. & JAN, L. Y. (1993). Primary structure and functional expression of a mouse inward rectifier potassium channel. *Nature* **362**, 127–133.

LAZARENO, S., BUCKLEY, N. J. & ROBERTS, F. F. (1990). Characterization of muscarinic M_4 binding sites in rabbit lung, chicken heart, and NG108-15 cells. *Molecular Pharmacology* **38**, 805–815.

MCLACHLAN, E. M. & MECKLER, R. L. (1989). Characteristics of synaptic input to three classes of sympathetic neurone in the coeliac ganglion of the guinea-pig. *Journal of Physiology* **415**, 109–129.

MAKHINA, E. N., KELLY, A. J., LOPATIN, A. N., MERCER, R. W. & NICHOLS, C. G. (1994). Cloning and expression of a novel human brain inward rectifier potassium channel. *Journal of Biological Chemistry* **269**, 20468–20474.

MARRION, N. V., SMART, T. G., MARSH, S. J. & BROWN, D. A. (1989). Muscarinic suppression of the m-current in the rat sympathetic ganglion is mediated by receptors of the m1-subtype. *British Journal of Pharmacology* **98**, 557–573.

MILLER, J. H., AAGAARD, P. J., GIBSON, V. A. & MCKINNEY, M. (1992). Binding and functional selectivity of himbacine for cloned and neuronal muscarinic receptors. *Journal of Pharmacology and Experimental Therapeutics* **263**, 663–667.

NORTH, R. A. & UCHIMURA, N. (1990). 5-Hydroxytryptamine acts at 5-HT_2 receptors to decrease potassium conductance in rat nucleus accumbens neurones. *Journal of Physiology* **417**, 1–12.

PERIER, F., RADEKE, C. M. & VANDENBERG, C. A. (1994). Primary structure and characterization of a small-conductance inwardly rectifying potassium channel from human hippocampus. *Proceedings of the National Academy of Sciences of the USA* **91**, 6240–6244.

SCHMIDT, R. E., MODERT, C. W., YIP, H. K. & JOHNSON, E. M. (1983). Retrograde axonal transport of intravenously administered ^{125}I-nerve growth factor in rats with streptozotocin-induced diabetes. *Diabetes* **32**, 654–663.

SKOK, V. I. & IVANOV, A. Y. (1983). What is the ongoing activity of sympathetic neurons? *Journal of the Autonomic Nervous System* **7**, 263–270.

STANFIELD, P. R., NAKAJIMA, Y. & YAMAGUCHI, K. (1985). Substance P raises neuronal membrane excitability by reducing inward rectification. *Nature* **315**, 498–501.

UCHIMURA, N. & NORTH, R. A. (1990). Muscarine reduces inwardly rectifying potassium conductance in rat nucleus accumbens neurones. *Journal of Physiology* **422**, 369–380.

WANG, H.-S. & MCKINNON, D. (1995). Potassium currents in rat prevertebral and paravertebral sympathetic neurones: control of firing properties. *Journal of Physiology* **485**, 319–335.

WEEMS, W. A. & SZURSZEWSKI, J. H. (1978). An intracellular analysis of some intrinsic factors controlling neural output from inferior mesenteric ganglion of guinea pigs. *Journal of Neurophysiology* **41**, 305–321.

WOODHULL, A. M. (1973). Ionic blockage of sodium channels in nerve. *Journal of General Physiology* **61**, 687–708.

Acknowledgements

We wish to thank Dr W. C. Taylor for the generous gift of himbacine and Drs Paul Adams, Ira Cohen and Shaul Hestrin for comments on the manuscript. This work was supported by grant NS-29755 from the National Institutes of Health and a grant from the American Heart Association.

Received 5 May 1995; accepted 11 November 1995.